Scour About a Single, Cylindrical Pile Due to Combined Random Waves and a Current

Robert W. Eadie, IV* and John B. Herbich,** M.ASCE

Introduction

There have been many studies of scour around piles caused by waves, and some studies of scour by waves and currents combined. However, almost all of the studies were conducted with monochromatic waves. The purpose of this investigation was to study what scouring effects various currents and random waves have on a single, cylindrical pile. These results were then compared with the results from previous studies of scour resulting from currents and monochromatic waves at Texas A&M University (Armbrust, 1982 and Wang, 1983).

Experiments were conducted in a two-dimensional wave tank. The pile used in this study had a diameter of 1.5 inches. Two water depths, four currents, one sediment size and four random wave spectra were utilized. Using data obtained from the experiments, an attempt was made to describe scour in terms of relevant dimensionless parameters.

Scour

The scour phenomenon begins with the incipient motion of sediment particles. Incipient sediment motion is defined to be "an instantaneous condition reached when the resultant of all the active forces on the particle intersects the line connecting the bed particle contact points," (Eagleson and Dean, 1961). There are three types of active forces acting on a sediment particle. Two of these forces, the drag and lift forces, are due to the fluid motion. These forces are in turn balanced by the sediment particle mass.

A thorough understanding of these forces is required in order to comprehend fully the processes of incipient motion, bedload transport and bed form development; all of which depend on the collective response of initially stationary bed particles to fluid forces.

In oscillatory flow generated by waves, the scour hole initiates at the side of the cylinder, and sometimes sediment deposition is found to occur against the upstream and downstream sides of the cylinder. Once fully developed, the scour hole is a radially symmetric frustrum of an inverted cone having side slopes at the angle of repose of the sediment (Palmer, 1969).

The mechanics of scour due to waves and currents are quite complicated and this type of scour occurs in almost all ocean environments. The

*Lt, CEC, U.S. Navy, Navy Experimental Diving Unit, Panama City, FL 32401.
**Professor, Civil and Ocean Engineering, Civil Engineering Department, Texas A&M University, College Station, TX 77843-3136.

scale and shape of the scour hole depends on the relative magnitude of the unidirectional velocity and the oscillatory flow velocities.

Experimental Study

Apparatus. Scour experiments were conducted in a 120-foot long (36.6 m), 3-foot deep (0.91 m) and 2-foot (0.61 m) wide, two dimensional, glass-walled wave flume. The test area was located approximately 40 feet (12.2 m) from the wave generator. The entire test area measured 40 feet (12.2 m) in length and was divided into several sections. An 8-foot (2.4 m) long, 5-inch (0.13 m) deep test sediment bed was bordered on each end by an 8-foot long (2.4 m) 10-inch (2.7 m) high false bottom. At the leading edge of the test area, a 16-foot (4.9 m) long ramp was used to gradually bring the wave up to the new depth at the top of the false bottom. A 1.5 inch (0.04 m) diameter aluminum pile was positioned along the centerline of the sediment bed.

Currents were produced using a centrifugal pumping system. The flow rate was monitored using a Fischer and Porter electromagnetic flow meter. The pump discharge entered the wave flume just forward of the wave generator and was diffused using a louvered grate. A Thermo-Systems model 1050 hot film anemometer was used to measure the vertical velocity distribution of the combined waves and currents.

The random wave generator used was a Seasim modular wave making system. This system consisted of a servo control system amplifier, a programmable spectrum random signal generator, an autocompensating wave height gauge and a paddle type sea wave simulation rolling seal modular wave generator.

A capacitance-type wave gauge was used with a Hewlett-Packard model 17403A carrier pre-amplifier to measure wave profile. To determine the significant wave height from the wave profile, a wave digitizer was used.

A wave absorber was positioned in the wave flume at the opposite end of the wave generator to reduce any reflections which might occur.

Scour depth readings were made using a point gauge after each test.

Procedures

A total of 20 experiments were performed. Four runs utilized currents only and the remainder used a combination of waves and currents. All test runs used a 1.5 inch (0.04 m) diameter pile placed in a bed of glass microbeads. The microbeads had a mean diameter (D_{50}) of 0.1 mm and a specific gravity of 2.45. Four different wave spectra were generated: Darbyshire, Pierson-Moskowitz, Jonswap (wave period = 8 secs) and Jonswap (wave period = 10 sec). Two water depths 0.917 ft (0.28 m) and 1.167 ft (0.36 m) and two different currents at each depth were employed, i.e. 0.380 fps (0.116 mps) and 0.650 fps (0.198 mps) at 0.917 ft (0.280 m), and 0.405 fps (0.123 mps) and 0.485 fps (0.148 mps) at 1.167 ft (0.036 m).

At the onset of each test, the sediment bed was leveled to a 5 inch (0.13 m) uniform thickness. After achieving the required water depth, the proper flow rate was established. The desired water level was maintained by regulating a 10-inch discharge valve located at the rear of the tank. The sediment bed was once again leveled as the above variables remained constant. The previously programmed signal generator then started generating the desired wave spectrum. Maximum scour depth was recorded at various intervals throughout each run, the time increment increasing as the test progressed. Each test was completed when equilibrium in the measured maximum scour depth was attained. After draining the tank, the patterns were photographed and sediment elevations, taken in the form of a rectangular grid, were established with the point gauge to determine equilibrium scour depth.

Results

Dimensionless Plots. There are many pertinent variables in a study of scour; the more important are: water depth (h), significant wave height ($H_{1/3}$), acceleration due to gravity (g), combined wave-current velocity (U), pile diameter (D), median sediment diameter (D_{50}), sediment/fluid density difference ($\rho_s - \rho$), density of water (ρ), kinematic viscosity of water (ν), and ultimate scour depth (S_d).

Since random waves were used in the study, and were defined by the significant wave height ($H_{1/3}$), wave period and wave length were omitted from the above list of variables. In the dimensional analysis, S_d was chosen as the unit of length, S_d^2/ν as the unit of time and $/S_d^3$ as the unit of mass. The remaining seven variables expressed in these units give the following dimensional numbers:

$$S_d/h,\ S_d/H_{1/3},\ S_d/D,\ S_d/D_{50},\ \rho/(\rho_s-\rho),\ \nu^2/S_d^3g,\ \nu/S_du$$

by rearranging and combining terms:

$$\frac{1}{(S_d/D)(\nu/S_du)}\ \frac{UD}{\nu} = N_{RP}$$

$$[(S_d/h)(1/(\nu/S_du)^2)(\nu^2/S_d^3g)]^{1/2} = u/\sqrt{gh} = N_F$$

$$[(S_d/D)(1/(\nu/S_du)^2)(\nu^2/S_d^3g)]^{1/2} = u/\sqrt{gD} = N_{FP}$$

$$[(1/2)(\nu 2/S_d^3g)(1/(\nu/S_du)^2)]^{1/2} = u/\sqrt{2S_dg} = N_{ES}$$

$$[(1/(\nu/S_du)^2)(\nu^2/S_d^3g)(S_d/D_{50})(\rho/(\rho_s-\rho))]^{1/2}$$
$$= U/\sqrt{gD_{50}((\rho_s-\rho)/\rho)} = N_S$$

Therefore, the functional relationship for scour is:

$$\frac{S_d}{h} = f(S_d/H_{1/3},\ S_d/D,\ S_d/D_{50},\ N_{RP},\ N_F,\ N_{FP},\ N_{ES},\ N_S).$$

On various dimensionless plots, data from experiments conducted by Armbrust and Wang were used in combination with data obtained from the random wave-current interaction experiments. Regression analysis was performed on the plots in order to construct the appropriate curves. Logarithmic regression analysis was used on the semi-logarithmic plots, and power regression analysis was used on the full logarithmic plots. The "r^2" term adjacent to each curve represents the correlation coefficient for each curve.

It was discovered that a relationship exists between scour depth and sediment number (N_S), (Figures 1 and 2) as well as between scour depth and the pile Reynolds number (N_{RP}), (Figures 3 and 4). However, scour depth is not dependent on N_S, or N_{RP} alone, but is also dependent on pile diameter as well as sediment size.

By plotting the relative scour depth (S_d/h) against the product of the pile Reynolds number and the sediment number $(N_{RP})(N_S)$, all data points collapsed onto a single curve regardless of variance in pile diameter or sediment size (Figure 5). It appears that since all data collapse onto a single curve, the type of wave train used for model studies, either monochromatic or random, is insignificant in the prediction of scour depth about a single cylindrical pile. However, the geometric shape of the scour hole differs with the type of wave train generated. By using a dimensionless plot (Figure 5), it appears as though predictions of scour depth could be made for situations in which the pile diameter or mean sediment size varied without utilizing scaling factors. Before any conclusions can be made, field data are required to evaluate the need, if any, for scale effects.

Scour Patterns. The rate of scour hole development by wave-current interaction was faster than that due to a steady current alone. Scour development is very rapid initially, the scour rate then decreases until the equilibrium scour depth is reached. Figure 6 shows a typical pattern of scour development in its initial stages, approximately the first 2 to 5 minutes of test. Figures 7 and 8 are the typical scour patterns that occur due to wave-current interaction 30 minutes and 2 to 3 hours after test commencement, respectively.

In all cases, the scour hole due to wave-current interaction was similar in shape to the scour hole formed by a steady current. This shape resembles an inverted cone. A typical example of a scour hole formed by a steady current is shown in Figure 9. Figures 10 to 13 depict the scour pattern formed by the same current used in Run 4 (Figure 8), combined with four different random wave spectra. As stated previously, the equilibrium scour hole associated with the wave-current interaction was deeper when compared to the equilibrium scour hole formed by a steady current alone. The size and shape of the equilibrium scour hole associated with wave-current interaction was at times greater than, approximately equal to, or less than the size and shape of the scour hole due to a steady current alone. These results differ from the prediction made by Niedoroda and Dalton in 1982. They stated that the scour hole

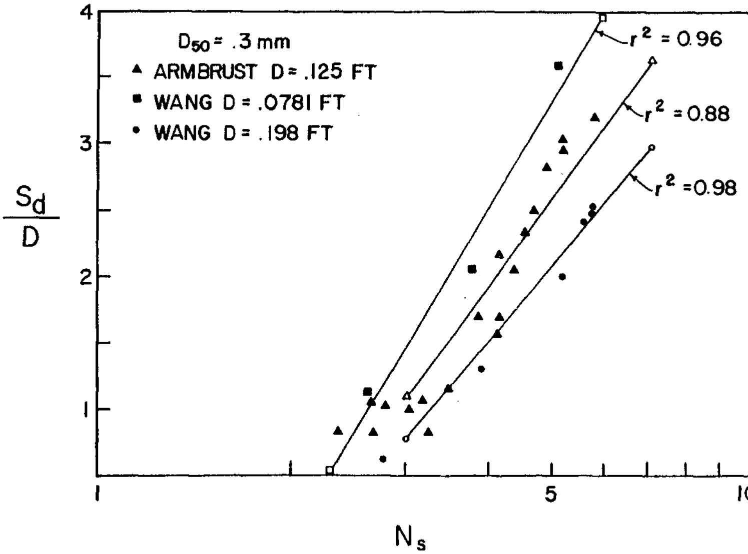

Figure 1. Relative scour depth, S_d/D, vs. sediment number for a constant sediment size and various pile diameters.

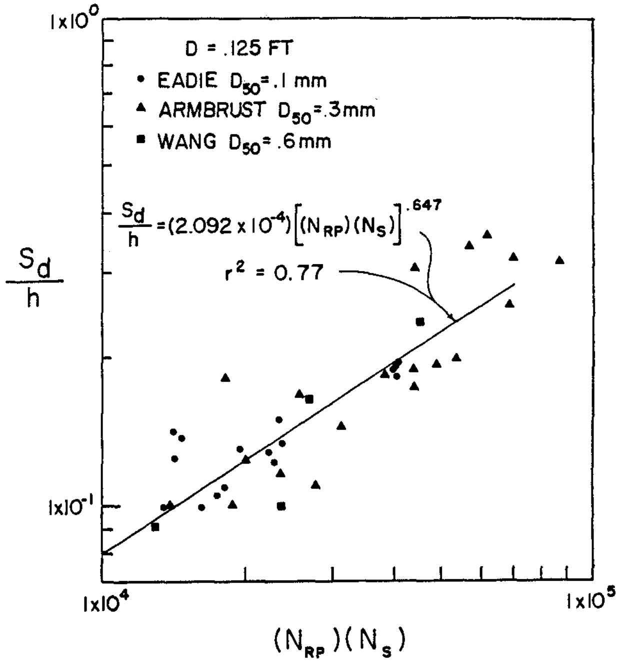

Figure 2. Relative scour depth, S_d/D, vs. sediment number times pile Reynolds number for a constant pile diameter and various sediment sizes.

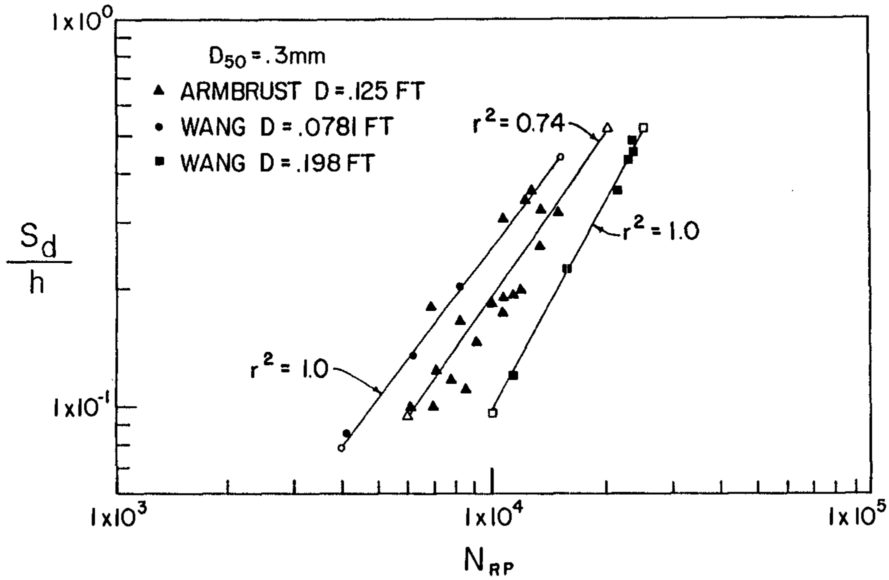

Figure 3. Relative scour depth, S_d/h, vs. sediment number times pile Reynolds number for a constant sediment size and various pile diameters.

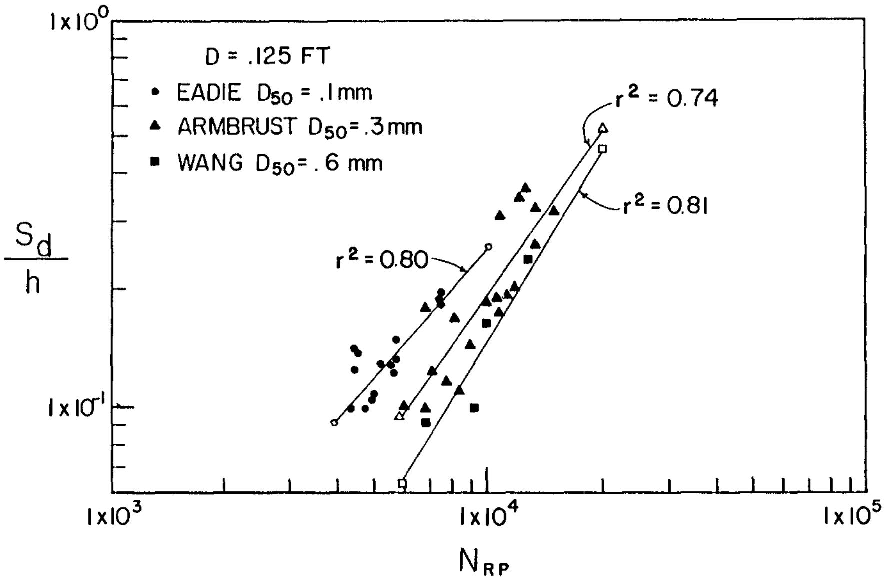

Figure 4. Relative scour depth, S_d/h, vs. pile Reynolds number for a constant pile diameter and various sediment sizes.

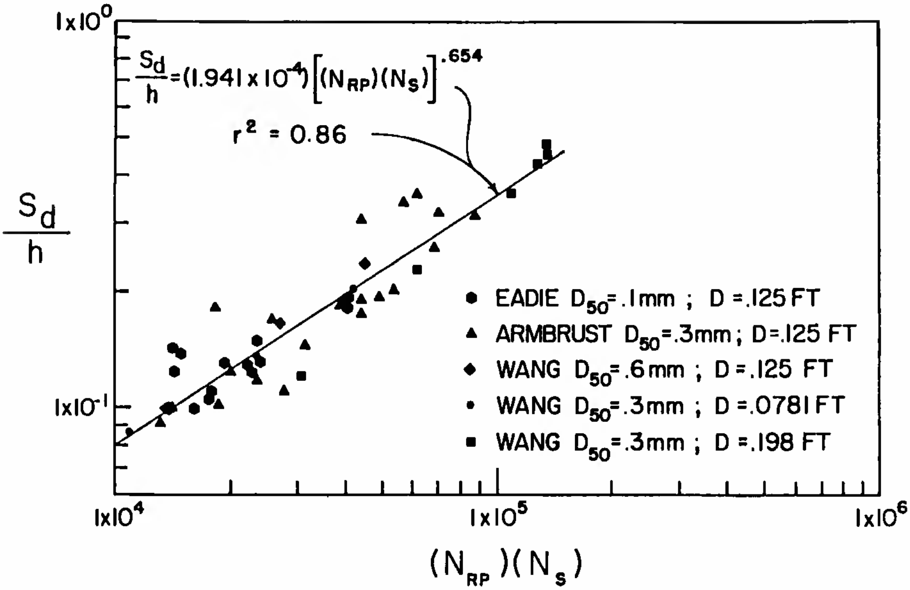

Figure 5. Relative scour depth, S_d/h, vs. sediment number times pile Reynolds number for various sediment sizes and pile diameters.

Figure 6. Initial stages of scour development.

Figure 7. Scour pattern 30 minutes after test commencement.

Figure 8. Scour pattern 2 to 3 hours after test commencement.

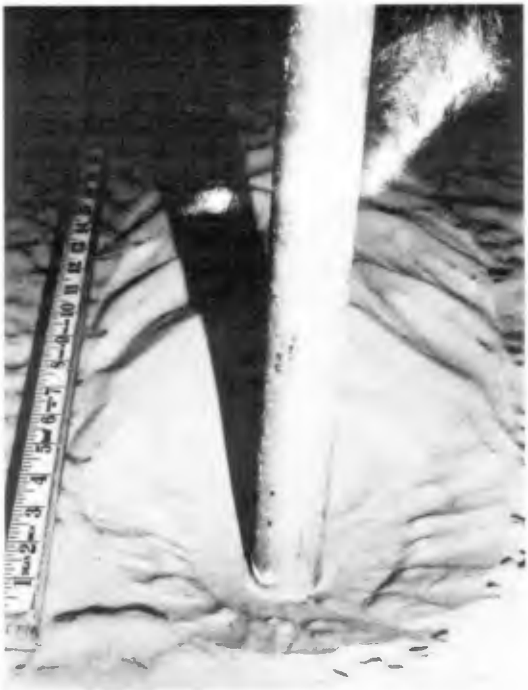

Figure 9. Typical scour cavity due to a steady current.
h=1.167 ft (0.36 m); U_c=.485 fps (0.148 mps); D=.125 ft; S_d=.14 ft (0.043 m)

Figure 10. Scour pattern due to random waves and current - Run 13.
h=1.167 ft (0.36 m); U_c=.485 fps (0.148 mps); U=.498 ft/sec (0.1518 mps); wave spectrum-Darbyshire; $H_{1/3}$=.1724 ft (0.053 m);D=.125 ft (0.038 m); S_d=.143 ft (0.044 m)

Figure 11. Scour pattern due to random waves and current - Run 14.
h=1.167 ft (0.36 m); U_c=.485 ft/sec (0.148 mps); U=.491 ft/sec (0.150 mps); wave spectrum=Pierson-Moskowitz; $H_{1/3}$=.1527 ft (0.047 m); D=.125 ft (0.038 m); S_d=.149 ft (0.045 m)

Figure 12. Scour pattern due to random waves and current - Run 15.
h=1.167 ft (0.36 m); U_c=.485 ft/sec (0.148 mps); U=.504 ft/sec (0.154 mps); wave spectrum=Jonswap (T=8 sec); $H_{1/3}$=.1631 ft (0.050 m); D=.125 ft (0.038 m); S_d=.174 ft (0.053 m)

Figure 13. Scour pattern due to random waves and current - Run 16.
h=1.167 ft (0.36 m); U_c=.485 ft/sec (0.148 mps); U=.508 ft/sec (0.155 mps); wave spectrum=Jonswap (T=10 sec); $H_{1/3}$=.1550 ft (0.047 m); D=.125 ft (0.038 m); S_d=.155 ft (0.047 m)

size and shape for combined waves and currents should not be as great as that developed by a steady current alone.

The general scour pattern was one of localized scour around the pile. A vortex formed around the pile due to disturbed flow and suspended the sediment. The sediment was carried farther downstream under the combined effects of waves and currents than it was with a steady current alone. Initially, the sediment suspension appeared to become greater as the scour hole developed, possibly due to a strengthening of the vortex system surrounding the pile. Because of the disturbance of flow caused by the pile, trailing ripples formed immediately behind the pile extending in the direction of wave propagation as the test progressed.

In all cases, the maximum scour depth occurred downstream of the pile, approximately 1/4 inch from the pile, and at an angle of approximately 40 degrees to the left or right of an imaginary line drawn through the pile and parallel with the wave flume walls.

Summary

1. Scour development was very rapid initially. The scour rate then decreased until an equilibrium scour depth was reached.

2. Scour development due to current and wave action occurred faster than scour due to a steady current alone.

3. The equilibrium scour depth caused by wave-current interaction is approximately 10 percent greater than the scour depth caused by a steady current alone.

4. The shape of the scour hole due to waves and currents and the shape of the hole due to current alone are similar. The shape resembles an inverted cone.

5. A relationship exists between scour depth and sediment number (N_S). However, scour depth is not dependent on N_S alone, but is also dependent on pile diameter and sediment size.

6. A relationship also exists between scour depth and the pile Reynolds number (N_{RP}). Again, scour depth is not dependent on (N_{RP}) alone, but is also dependent on pile diameter, as well as sediment size.

7. By plotting the relative scour depth (S_d/h) against the product of the pile Reynolds number and sediment number, (N_{RP}) (N_S), all data points collapse onto a single curve regardless of variance in pile diameter or sediment size.

Although the amount of data is limited, due to the fact that all data could be collapsed onto one curve when plotting S_d/h versus (N_{RP})(N_S), (Figure 5), it appears as though the type of wave train used for model studies, either mono-chromatic or random, is insignificant in the prediction of scour depth about a single, cylindrical pile. However, when attempting to predict the geometry of the scour hole, the irregularity of the wave train becomes very significant. Armbrust stated that the pattern of scour for wave-current interaction is no longer conical in shape, but the pattern is irregular due to the wave particle orbital motion. The data in this study clearly indicate a conical scour pattern for random wave-current interaction. Although these results are different from those of Armbrust, they agree with field data, as well as with the predictions of Niedoroda and Dalton. The fact that the geometric shape of the scour hole differs with the type of wave train used, may become important in the prediction of scour depth around multiple pile cases.

The conclusions resulting from this study were found for a flow in which the steady current was greater than the oscillatory flow produced by the waves. If the magnitude of the two flows in relation to one another change, the flow patterns will also change and the geometry of the scour hole may very likely differ from results found in this study.

References

Armbrust, S.F. (1982). Scour about a cylindrical pile due to steady and oscillatory motion. Master's Thesis, Texas A&M University.

Eagleson, P.S. and Dean, R.G. (1961). Wave induced motion of bottom sediment particles. Transactions, ASCE, Vol. 126:1162-1189.

Herbich, J.B., Schiller, R.E., Jr., Watanabe, R.K., Dunlap, W.A. (1984). SeaFloor Scour: Design Guidelines for Ocean-Founded Structures, Marcel Dekker, Inc., New York and Basel.

Niedoroda, A.W. and Dalton, C. (1982). A review of the fluid mechanics of ocean scour. Ocean Engineering, 9(2):159-170.

Wang, R.K. and Herbich, J.B. (1983). Combined current and wave-produced scour around a single pile. COE Report No. 269, Texas A&M University.

List of Notations

Symbol	Quantity	Units	Dimensions
D	pile diameter	ft	L
D_{50}	mean diameter of sediment	ft	L
h	still water depth	ft	L
$H_{1/3}$	significant wave height	ft	L
N_{RP}	pile Reynolds number = UD/ν	-	-
N_s	sediment number = $U/\sqrt{gD_{50}[(\rho_s-\rho)/\rho]}$	-	-
S_d	ultimate scour depth	ft	L
T	wave period	sec	T
U	mean wave-current velocity	ft/sec	L/T
U_c	current velocity	ft/sec	L/T